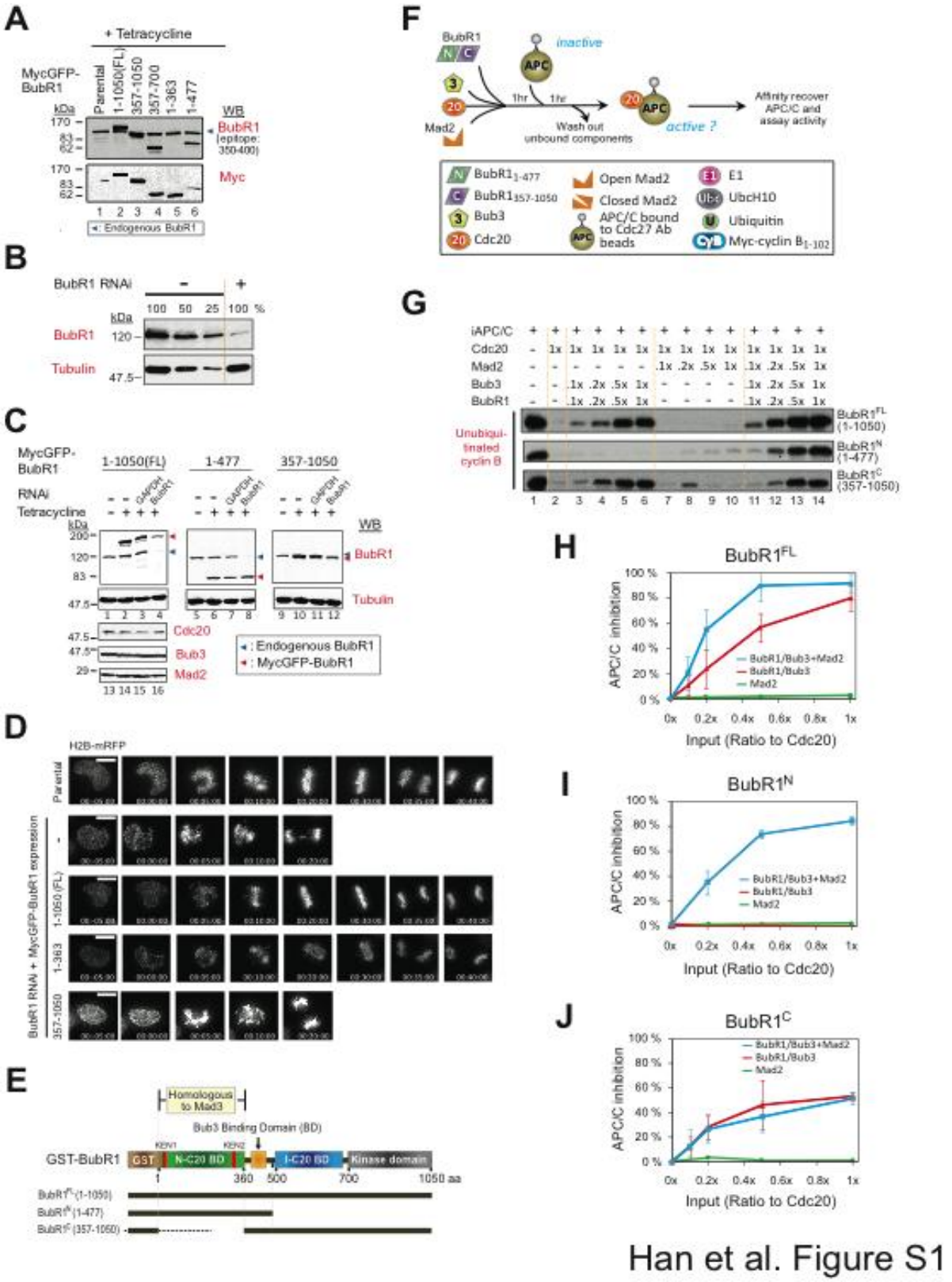

Han et al. Figure S1

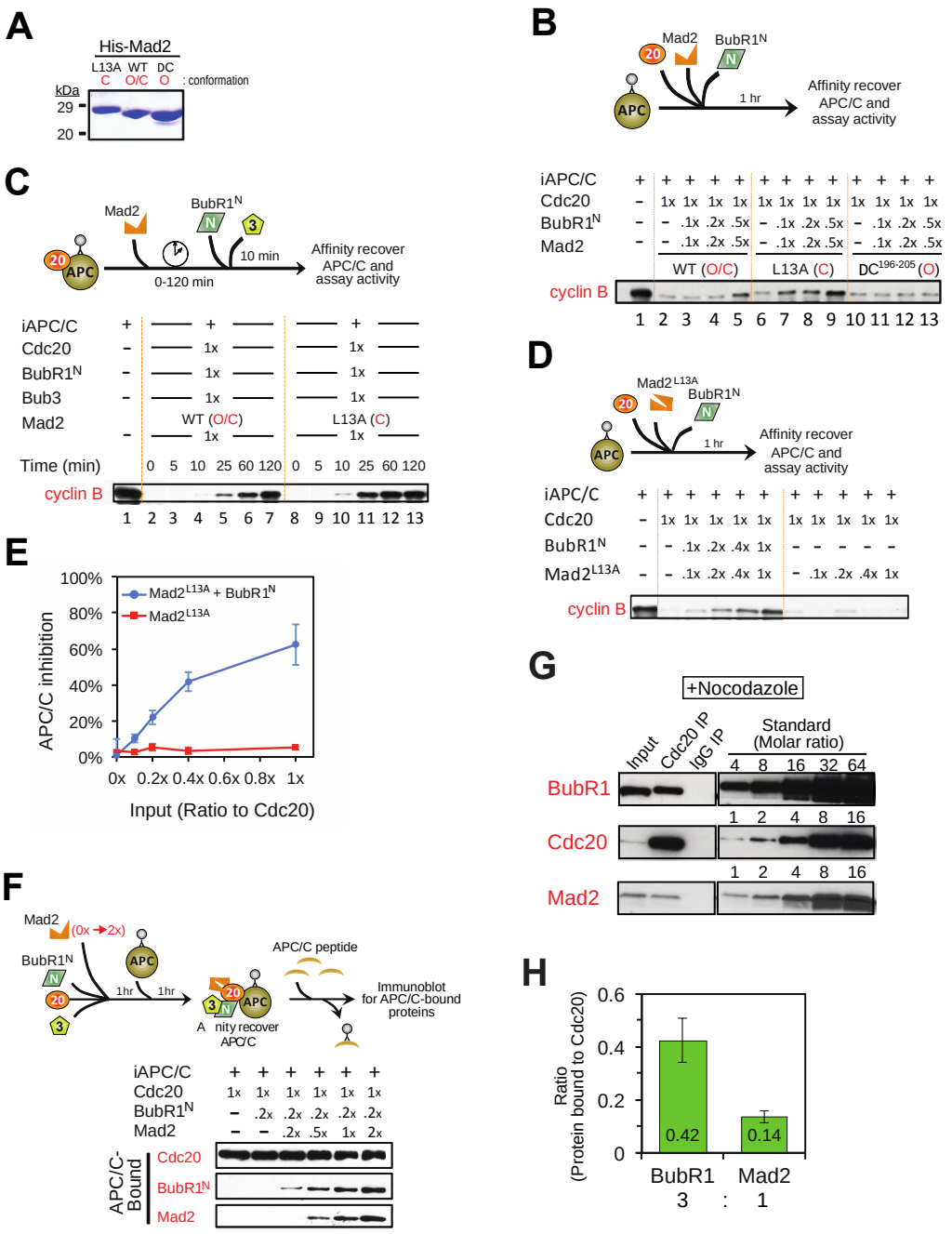

Han et al. Figure S2

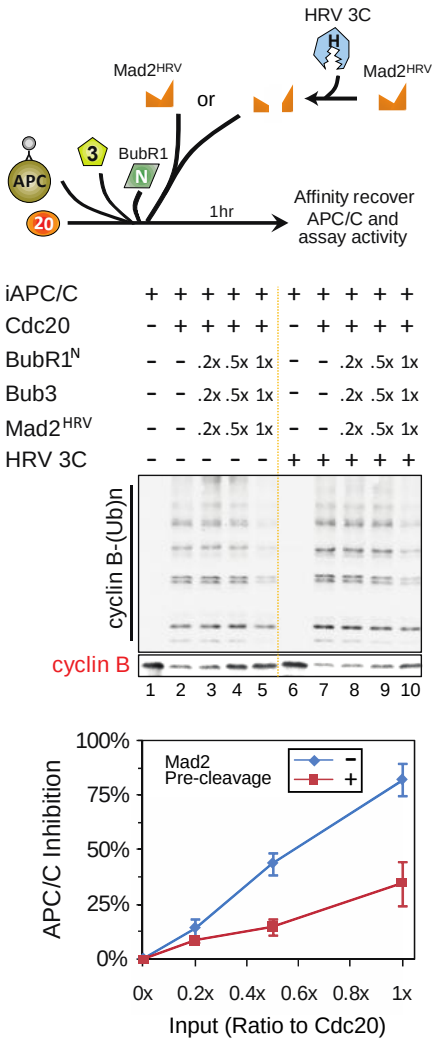

Han et al. Figure S3

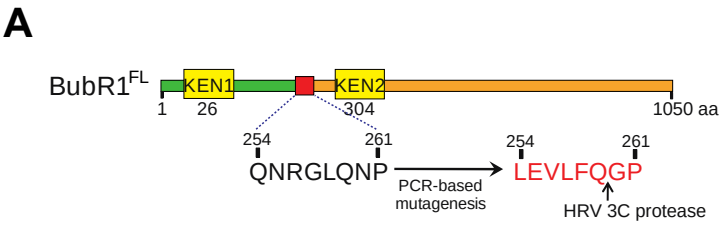

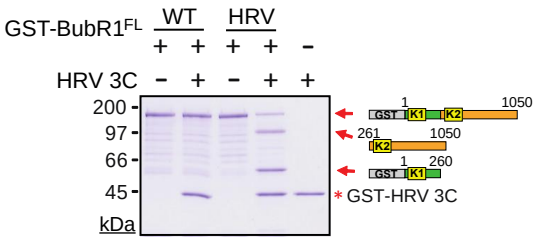

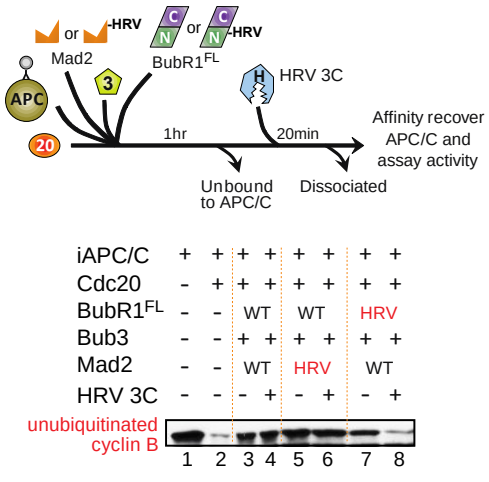

Han et al. Figure S4

A

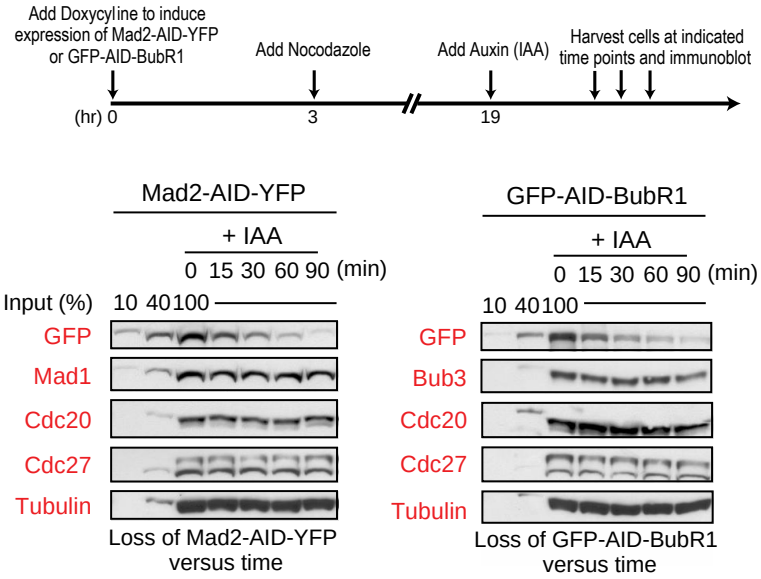

B

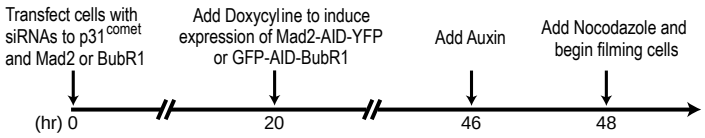

C

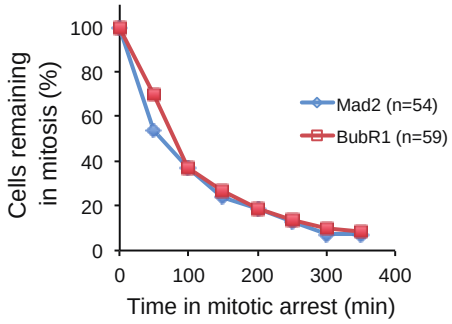

Han et al. Figure S5

SUPPLEMENTAL INFORMATION

Figure S1. BubR1's Mad3 homology domain Cdc20 binding site is required for the Mad2-dependent mitotic checkpoint signaling in vivo and in vitro (*related to Figure 1*).

(A) Immunoblot showing tetracycline-induced expression of various MycGFP-BubR1 transgenes. Endogenous BubR1 is indicated by blue arrowhead. Note that MycGFP-$BubR1_{1-363}$ signal is missing in the BubR1 blot (top panel) due to the absence of the epitope in the fragment. **(B)** Efficient removal of endogenous BubR1 by transfection into HeLa cells of an siRNA targeting 3' untranslated region of the BubR1 mRNA. Dilutions of untransfected cells are used to validate that ~90% of endogenous BubR1 is lost by 48 hour post-transfection. **(C)** Replacement of endogenous BubR1 with various MycGFP-BubR1 proteins after HeLa cells were transfected either by control (GAPDH) siRNA or an siRNA targeting the 3' untranslated region of the BubR1 mRNA to selectively deplete endogenous BubR1. Stably integrated genes encoding BubR1 variants were expressed by addition of tetracycline 24 h after siRNA transfection. Cells were collected and analyzed for immunoblotting. Endogenous BubR1 (blue arrowhead) and MycGFP-BubR1 (red arrowhead) signals are indicated. Levels of other checkpoint components such as Bub3, Mad2, and Cdc20 were not affected by the transfection. **(D)** Representative still images of mitotic progression in cells of which BubR1 was replaced with either full-length or fragment of MycGFP-BubR1. Cells were imaged by time-lapse microscopy every 5 min from nuclear envelope breakdown. Chromosomes were visualized by histone H2B-mRFP. Time is marked in the bottom right of each panel. Scale bar = 10 μM. **(E)** Schematic of GST-BubR1 variant constructs for Baculoviral expression and purification. **(F-J)** Inhibition of Cdc20 *in vitro* by BubR1 variants with Bub3 and Mad2. **(F)** Schematic of APC/C ubiquitination activity assay. **(G-J)** Assays of

BubR1^{FL}, BubR1^{N} and BubR1^{C} for inhibition of Cdc20 activation of APC/C. **(G)** APC/C activity (quantified by depletion unubiquitinated cyclin B) was assessed after co-incubation of increasing amounts of the individual BubR1 variant, Bub3, Mad2, and Cdc20 prior to further incubation with APC/C. **(H-J)** Plots showing percent inhibition of APC/C activity from assays in **(G)**, with **(H)** BubR1^{FL}, **(I)**, BubR1^{N}, and **(J)** BubR1^{C}. Error bars represent SEM (n=3).

Figure S2. The closed conformation of Mad2 promotes the binding of BubR1's N-terminus to Cdc20 to inhibit its activation of APC/C (*related to Figure 2*).

(A) Purified Mad2 variants (L13A, WT, ΔC), assessed by Coomassie staining. **(B)** Experimental data for Fig. 2A. **(C)** Experimental data for Fig. 2B. **(D)** Closed Mad2 alone does not inhibit Cdc20 activation of APC/C. APC/C was incubated with increasing Mad2^{L13A} and Cdc20 in the presence or absence of increasing BubR1^{N}. APC/C activity assay were then performed as earlier. **(E)** Plots show the mean of percent APC/C inhibition from three independent assays. Error bars represent SEM. **(F)** Mad2-dependent BubR1 loading onto APC/C^{Cdc20}. ***(Top)*** Schematic of assay to determine checkpoint proteins bound to APC/C. Bead-bound APC/C was incubated with BubR1^{N}, Cdc20, and increasing amount of Mad2, recovered, peptide-eluted from Affiprep beads, and analyzed for bound components by immunoblotting ***(Bottom)***. **(G)** Immunoprecipitation of Cdc20 from nocodazole-induced, mitotically arrested HeLa cells. A dilution series of purified proteins was used to quantify the amounts of BubR1 and Mad2 associated with Cdc20. **(H)** Quantitation of three independent experiments from (G), plotted as the molar ratio compared with associated Cdc20. Error bars represent SEM.

Figure S3. Pre-digestion of Mad2^{HRV} impairs Mad2-dependent BubR1^{N} inhibition of APC/C^{Cdc20} *(related to Figure 3)*.

(Top) Schematic of experimental design. APC/C and Cdc20 were incubated with increasing amounts of BubR1^{N}, Bub3, and Mad2^{HRV} (either pre-digested by HRV 3C protease or not), followed by APC/C purification and activity assay. ***(Middle)*** APC/C activity assays for ubiquitination of cyclin B. **(*Bottom*)** Quantification of the mean of percent APC/C inhibition from three independent experiments. Error bars represent SEM.

Figure S4. BubR1, but not Mad2, is the effector for APC/C^{Cdc20} inhibition *in vitro* *(related to Figure 4)*.

(A) Diagram of cleavable BubR1^{FL} construct that is engineered to contain a HRV 3C recognition sequence between amino acids 254-261, residing between two KEN boxes. **(B)** HRV 3C-mediated digestion of the cleavable BubR1^{FL} *in vitro*. Cleavable BubR1^{FL} was incubated at room temperature for 20 min in the presence or absence of HRV 3C prior to analysis. **(C)** Assay to determine whether BubR1^{FL} or Mad2 is an effector for APC/C^{Cdc20} inhibition. Bead-bound APC/C was incubated with combinations of BubR1$^{FL\text{-}WT}$ or BubR1$^{FL\text{-}HRV}$, Bub3, Mad2^{WT} or Mad2^{HRV} and Cdc20, followed by removal of components unbound to APC/C. Buffer either containing HRV 3C protease or not was added and incubated for 20 min prior to APC/C-mediated cyclin $B_{1\text{-}102}$ ubiquitination.

Figure S5. The residual Mad2-AID-YFP or GFP-AID-BubR1 after IAA-induced degradation is not sufficient to enable sustained mitotic checkpoint signaling *(related to Figure 5)*.

(A) Mitotic degradation of Mad2-AID-YFP and GFP-AID-BubR1. Cells were treated with Doxycycline (1μg/ml) and Nocodazole (100 ng/ml) for 16 hours. After IAA (500 μM) addition, cells were harvested at indicated time points and analyzed by immunoblotting. **(B)** Schematic of the protocol for depletion of endogenous $p31^{comet}$ and Mad2 or BubR1 by siRNA transfection and induction of AID-tagged Mad2 or BubR1. IAA-induced degradation of AID-tagged Mad2 or BubR1 was performed in cells arrested in mitosis with nocodazole. **(C)** Time-lapse microscopy was used to determine the duration of mitosis in the presence of nocodazole (100 ng/ml) after IAA-induced degradation of Mad2-AID-YFP or GFP-AID-BubR1.